ISTITUTO NAZIONALE DI FISICA NUCLEARE

Sezione di Lecce

INFN/AE-96/07
26 Marzo 1996

G. Cataldi, F. Grancagnolo, S. Spagnolo:

CLUSTER COUNTING IN HELIUM BASED GAS MIXTURES

Submitted to
Nuclear Instrumentation and Methods in Physics Research

SIS-Pubblicazioni
dei Laboratori Nazionali di Frascati

INFN - Istituto Nazionale di Fisica Nucleare
Sezione di Lecce

INFN/AE-96/07
26 Marzo 1996

CLUSTER COUNTING IN HELIUM BASED GAS MIXTURES

G. Cataldi, F. Grancagnolo, S. Spagnolo

INFN–Sezione di Lecce, Via Arnesano, 73100 Lecce, Italy

Abstract

The statistical advantages deriving from counting primary ionization, as opposed to the conventional energy loss measurement, are extensively discussed. A *primary ionization counting method* is proposed for a 'traditional', cylindrical, single sense wire cell drift chamber, which makes use of a helium based gas mixture. Its conceptual feasibility is proven by means of a simple Monte Carlo. A counting algorithm is developed and tested on the simulation output. A definition of the parameters of the read out and of the digitizing electronics is given, assuming the described counting algorithm applied to a general detector design, in order to have a complete and realistic planning of a cluster counting measurement. Few interesting results from a dedicated test beam on primary ionization measurements and on π/μ separation are finally shown.

1 Introduction

Particle identification in high energy physics experiments is a difficult task. It often requires dedicated detectors to improve on the reliability of the off-line tagging techniques. The tracking devices, like drift or proportional chambers, can provide a measurement of the energy loss along the particle trajectory which, together with a measurement of the momentum, allow to infer the mass of the ionizing particle. The large and inherent uncertenties in total energy deposition represent, however, a serious limit to the particle separation capabilities. Primary ionization, on the other hand, thanks to its poissonian nature, offers a more statistically significant way to infer a mass information with no other tool than the tracking detector itself, and hence without affecting the transparency of the apparatus.

Section 2, starting from a summary of the theory of energy loss, is devoted to a comparison between these two different approaches to the particle ID problem. In section 3 the inherent technical difficulties related to cluster counting are presented along with suggestions to overcome them even in detectors like 'traditional' single sense wire drift chambers without recurring to dedicated 'ad hoc' geometries like the *time expansion chamber*[1]. A conceptual experiment is hence sckeched in order to illustrate the most relevant parameters in a cluster counting measurement. Section 4 describes a simple Monte Carlo, implemented to study the effects of the detector geometry and to prove the conceptual feasibility of the method. A counting algorithm is then proposed. Its reliability has been verified on the simulation output and it is used to determine the optimal parameters for the cluster counting measurement in the adopted setup. Finally, results from a dedicated beam test are illustrated in section 5: primary ionization measurements for minimum ionizing particles in He-Hydrocarbon mixtures are presented, the dependence of the number of clusters on the particle momentum is shown and π/μ separation for different momenta is attempted and compared to results achievable by the 'traditional' dE/dx truncated mean approach.

2 Primary ionization counting versus total energy loss measurement

2.1 A summary of energy loss mechanisms

The process of energy loss of charged particles traversing a medium, although described in terms of continuous and macroscopic variables, is essentially discrete in nature. It consists, in fact, in a sequence of isolated interactions of the ionizing particle with the atoms, or the molecules of the medium, like excitation and ionization, or elastic scattering processes (like Rutherford scattering) involving free electrons.

The relative importance of these processes can be influenced by secondary effects depending on the nature of the medium. The energy transfer spectrum for a single collision has a typical trend, where one can qualitatively mark out three regions: a) a low energy region (extending up to the mean ionization potential and where one-half of all interactions fall) extremely rich in structures, related to the multiple discrete energetic exctitation levels available for the medium; b) a high energy region (extending up to the maximum kinematically allowed energy transfer in a collision with atomic electrons: $\sim 2m_e\gamma^2v^2$) which, as suggested by the E^{-2} trend, characteristic of elastic scattering processes, comes from close

collisions between the particle and the atomic electrons. Here there are no traces of the atomic binding of the electrons because of a momentum transfer much greater than the binding energy; c) an intermediate energy region, where the main process is the ionization from distant interactions of the particle with the whole atom.

The most important feature of the energy transfer spectrum is the long tail, which gives a not negligible probability of energy transfers well above the average.

The ionization which is produced during this phase of the energy loss process, commonly referred as *primary ionization*, is well separated, as far as the production mechanism is concerned, from the *secondary ionization*. The latter results from the subsequent energy degradation of ions and excited atomic states which are produced in the primary interaction. The total ionization comes from several different and extremely complex physical processes: a) ionization of an excited atom requiring less energy than the first ionization energy; b) ionization in collisions involving an excited atom of the same or of a different kind with respect to the ionized one. These interactions fall in the category of the so-called Penning and Jesse [2] effects and they strongly depend on the gas mixture. Sometimes metastable levels in the reaction chain can produce secondary ionizations delayed with respect to the primary process; c) ionization in collisions between energetic primary electrons and atoms of the gas, which strongly depend on the energetic distribution of the primary electrons and on the gas properties. The electron range determines the spatial spread of the secondary ionization around the primary ion production site. A borderline case is $\delta-$ray production along the particle track.

The final effect of the passage of a charged particle in a gas is, then, a track of ionization consisting in a sequence of clusters of one or more electrons which are all released in a single act of primary ionization. They are, generally, spatially confined thanks to a favourable ratio between the mean free path of the particle and the average range of primary electrons.

The relevant parameters for the description of this localized energy deposit are *primary ionization density* along the track and *cluster size*. The number of electrons belonging to each cluster depends on the energy released in the collision. The collisions which contribute to secondary ionization are those in which the ionized electrons are liberated with a kinetic energy larger than the first ionization potential I_0. However, for a given energy of the primary electron, the probability of ionization in subsequent collisions depends on the balance between the cross sections of elastic scattering σ_{es}, of ionization in distant collisions σ_i and of excitation σ_e. While σ_i is zero for energies lower than the first ionization potential, σ_e is small but not negligible for energy around and above I_0.

Theoretical evaluations of cluster size distributions have been made through Monte Carlo simulations in Argon [3]. The main inputs for such simulations consist in the photo-absorption cross section and in the cross sections for the various processes triggered by the collisions of low energy electrons in the gas. From the photo-absorption cross section one obtains the complex dielectric constant of the material, which describes the energy absorption and, thus provides the energy transfer spectrum [4],[5]. The cross sections for the electron collisions with the gas (σ_{es}, σ_i and σ_e) give the probability that the kinetic energy of the primary electrons can be used in secondary ionizations. Experimental cluster size determinations in Argon [6] agree with the Monte Carlo results. This theory provides, also, the dependence on the particle velocity of the total energy loss according to the traditional treatment by Bethe and Bloch. This is expressed by a trend dominated by a β^{-2} term up to a minimum at $\beta\gamma = 4$, where it begins a slow logarithmic rise due to the relativistic deformation of the Coulomb field, which increases the volume where the particle interacts in a not negligible way. Finally the material polarization generates a

screening of the ionizing particle charge inducing a saturation of the rise of energy loss (fig. (1)).

2.2 Statistical considerations

Primary ionization is a typical poissonian process. It is the final result of a large number, of the order of the Avogadro number, of very unlikely independent random events: the ionizing collisions. Their sum gives rise to the mean specific primary ionization N_{cl}. The number of randomly distributed clusters K along a track of length l fluctuates around $K_0 = lN_{cl}$ with a probability described by the well known relation:

$$P(K;K_0) = \frac{e^{-K_0}(K_0)^K}{K!} \tag{1}$$

The main advantage of the poisson probability distribution is that its gaussian limit is achieved as soon as the mean value approaches ~ 20, which is of the order of 1 *cm* track length for most of the commonly used gas mixtures. Furthermore, eq. (1) assures that the resolution of the measurement improves when the value of K_0 increases, that is, for a given gas mixture, when the track length increases. The obvious result is an inverse proportionality between the relative resolution, σ/K_0, and $l^{1/2}$.

The poissonian behaviour of the primary ionization has suggested the commonly used method for the measurement of the mean cluster density N_{cl}: the *inefficiency method.* It is based on the probability of having no signal in a triggered event, for a detector with gas thickness of unitary length, that is $e^{-N_{cl}}$. The inefficiency of such a detector is, hence, directely related to the cluster density in the gas.

The power of the poissonian behaviour of the primary ionization appears more evident when compared to the features of the Landau distribution function, which describes the fluctuations of the total energy loss. Owing to the large number of different processes, which contribute to the total energy loss of a charged particle, each one of them intrinsically and widely fluctuating, the statistical distribution of the energy loss is an extremely difficult function. While statistical considerations imply that the distribution of the energy loss in thick and dense materials has a gaussian shape, because of the very large number of ionizing collisions (central limit theorem), in gaseous materials, as in drift or proportional chambers, such considerations are of little or no help.

From an analytical point of view, the probability $f(E_0, E, x)$ that an ionizing particle of initial energy E_0 has an energy E at a depth x is defined by the following equation [7]:

$$\begin{aligned} f(E_0, E, x+dx) - \quad f(E_0, E, x) = -f(E_0, E, x)dx \int_0^{+\infty} dE' \Phi_{coll}(E, E') + \\ dx \int_0^{+\infty} dE' \Phi_{coll}(E+E', E') f(E_0, E+E', x) \end{aligned} \tag{2}$$

where the probability $\Phi_{coll}(E, E')$ that in a single collision the particle of energy E loses a quantum of energy E', is computed, as described above, from the cross sections of all the processes taking place in the medium. Analytical [8] and numerical [9] attempts to solve equation (2) have been made. The results refer to different regions in the energy transfer spectrum. They agree, also with more recent computations [4], on a broad and strongly asymmetric distribution, with a mean value openly grater than the most probable value of dE/dx. Its FWHM ranges from 60% to 100% of the most probable value. Furthermore the distribution is almost invariant on the track length, since the number of primary collisions, releasing a large amount of energy, and so allowing for $\delta-$ray production, becomes larger as the thickness of the traversed gas increases.

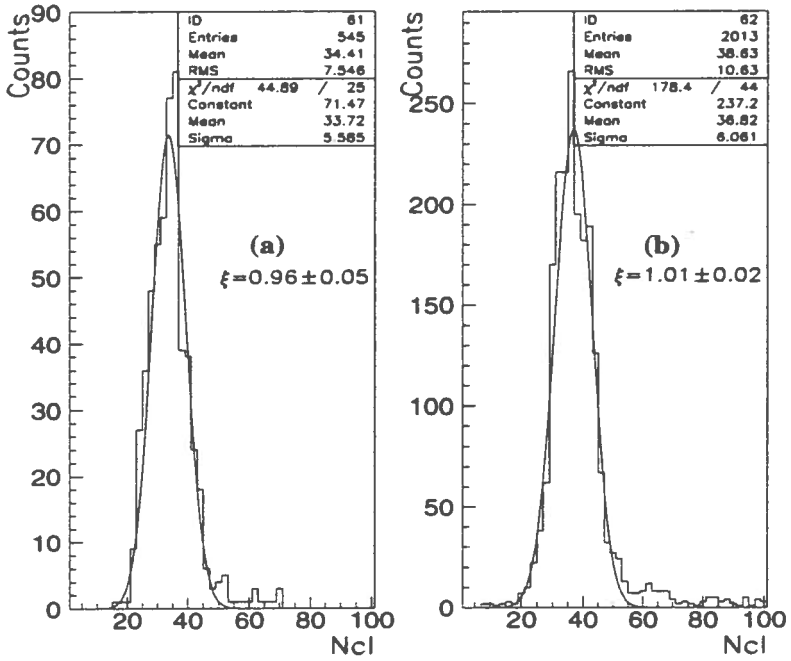

Fig. 12 Distribution of the number of clusters after an iterative application of the correction factor. The pion beam has a momentum of $280 MeV/c$. Two different mixtures are shown: (a) $80\%He - 20\%CH_4$ and (b) $95\%He - 5\%i\ C_4H_{10}$.

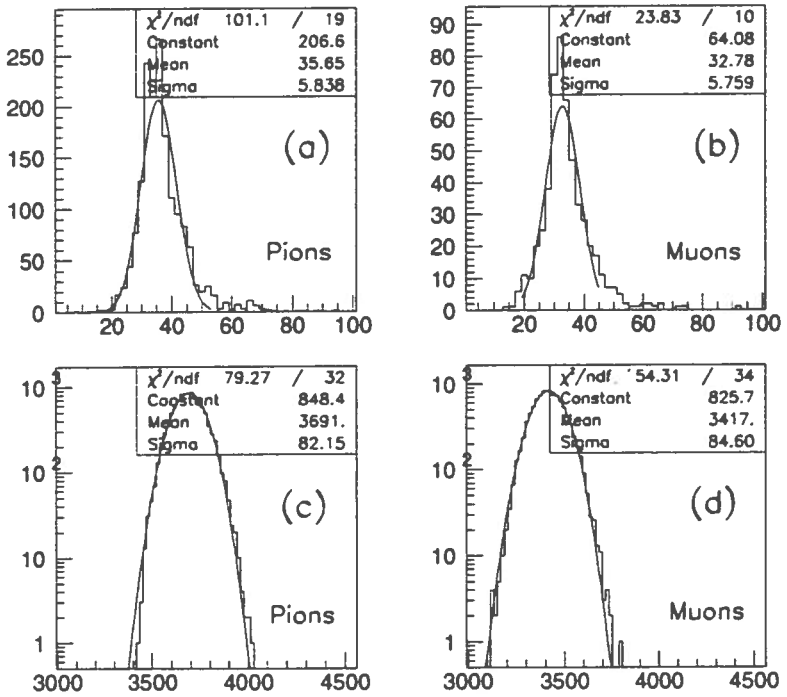

Fig. 13 Cluster distributions from single cell measurements ((a) pions, (b) muons) and for 100 cells sampling a track ((c) pions, (d) muons). Data refer to $200 MeV/c$ beam momentum and $95\%He - 5\%iC_4H_{10}$ gas mixture.

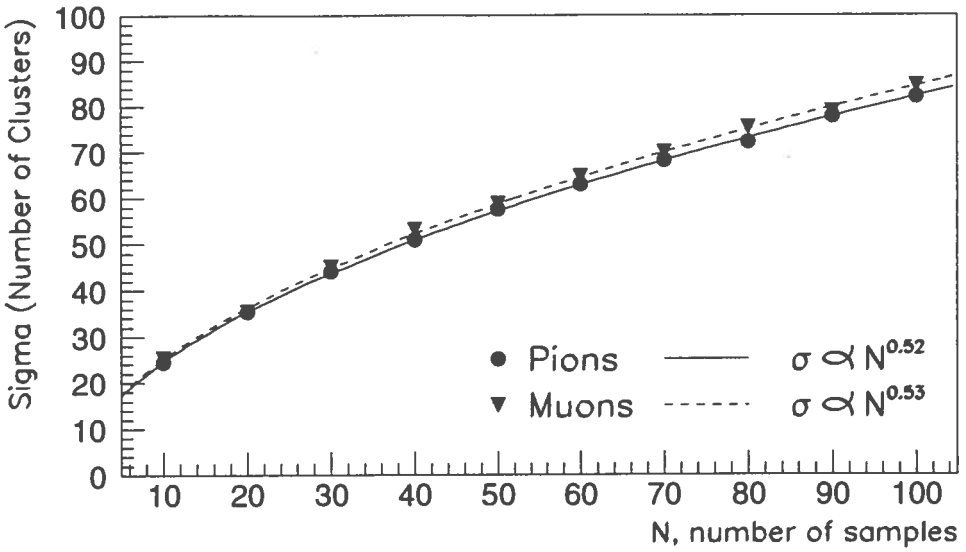

Fig. 14 Cluster counting resolution as a function of the track sampling.

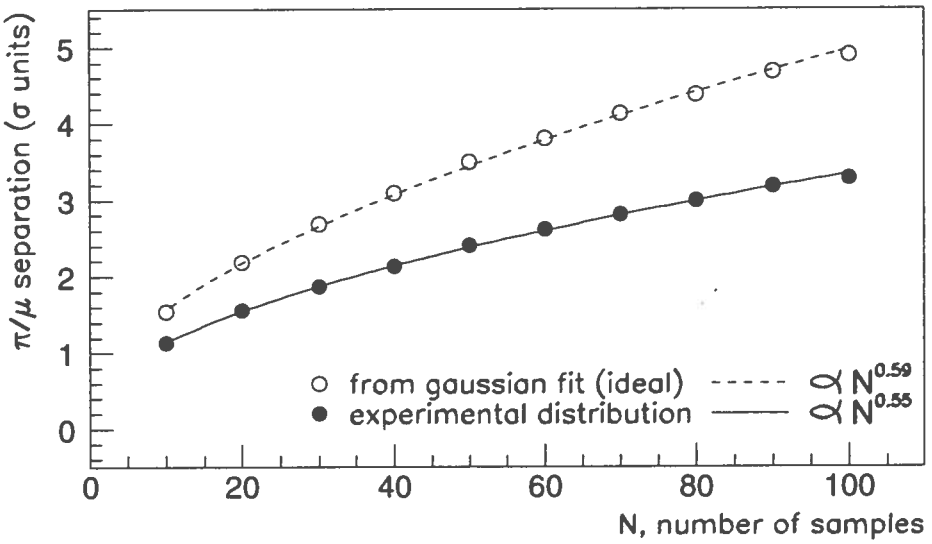

Fig. 15 π/μ separation from a cluster counting measurement as a function of the track sampling. For comparison the ideal cluster counting separation is superimposed.

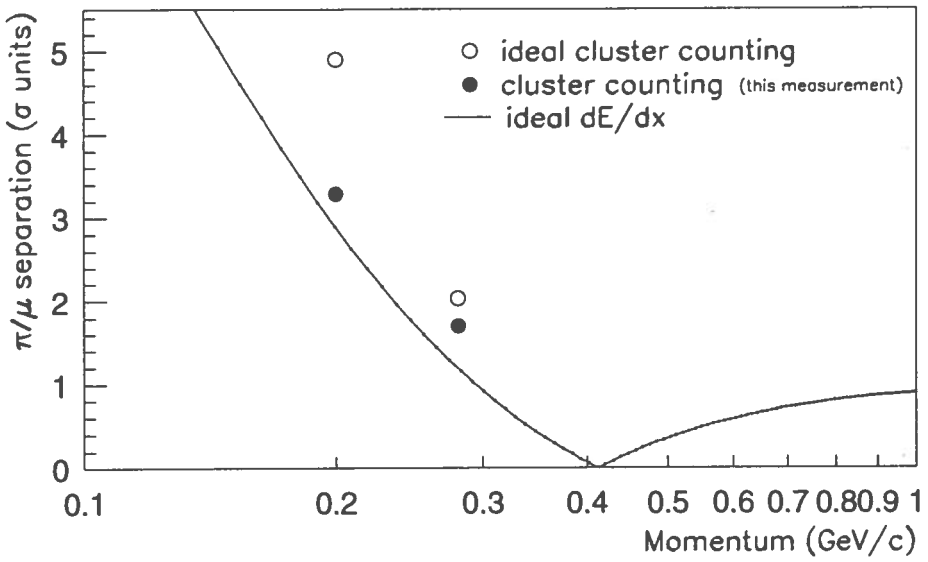

Fig. 16 π/μ separation as a function of the particle momentum. The solid line is an empirical extrapolation from existing data.

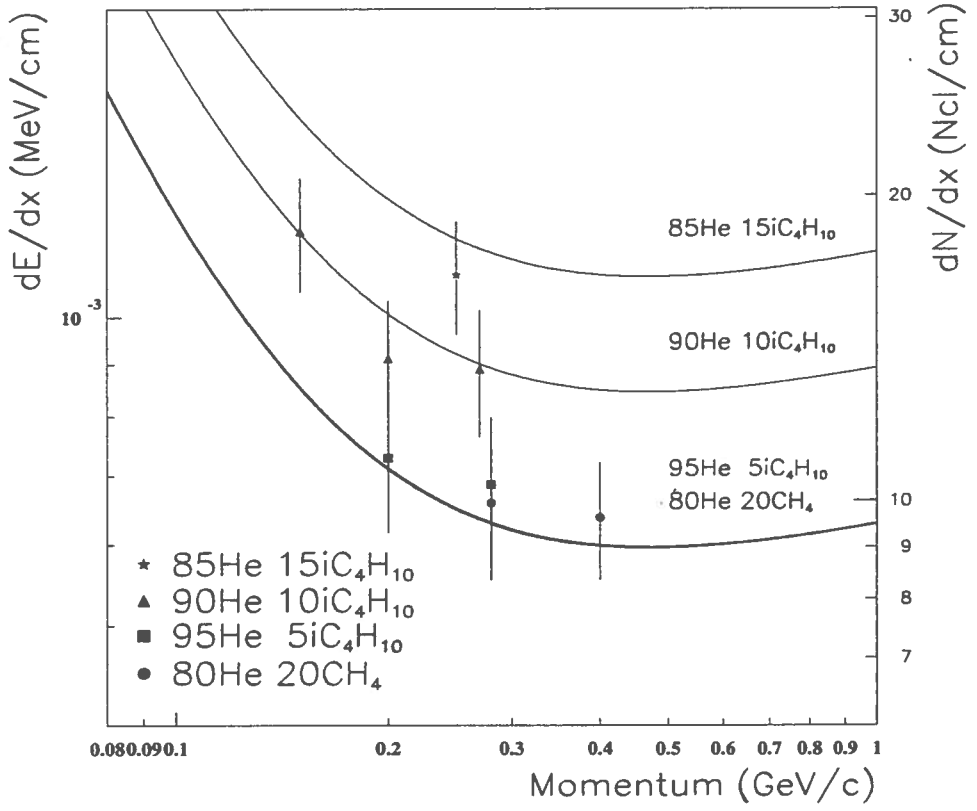

Fig. 17 Bethe-Bloch parametrization of dE/dx for pions, superimposed to the experimental data.

When one tries to use the total energy loss measurement for particle identification purposes, even in the most favourable momentum region (the relativistic rise) the typical separation between energy loss curves relating to different particles is smaller than the spread around the relative mean values. A satisfactory signal separation requires mass resolutions well below the inherent limit of the total energy loss.

From the above considerations it follows that there is an enormous statistical advantage in counting the primary ionization instead of the measurement of the total ionization. Neverthless the technical difficulties related to cluster counting have favoured dE/dx as a way to recognize particles of different nature, driving, as a consequence, the development of several methods to improve the achievable resolution.

These methods rely on a fine sampling of the ionization along the particle trajectory. Since the momentum loss, when traversing a gaseous material, is negligible and doesn't give rise to a relevant change in specific energy loss, all the measurements performed along the track can be treated as coming from a single energy loss distribution. A fit to the expected spectrum provides the best estimate of the most probable value of energy loss. The method of the trouncated mean allows to overcome the problems arising from the accurate evaluation of the theoretical distribution and from the need of a very large sample size. It works as a selective mean rejecting a certain percentage of the highest values of dE/dx in the collected sample. In this way the interactions involving large energy transfers, which are poor of informations about the particle velocity, do not contribute to the final measurement. The obtained mean represents the most probable value of the total ionization and the suppression of high energy tranfers results in an overwhelming gain in resolution. However, a number of sampling exceding 100 over a track length of the order of 2-3 meters is needed to achieve reliable particle separations. Experimental dE/dx resolutions in the range 2.5% $-$ 15% have been achieved with different average track lenghts (from $\sim 0.5\ m$ to $\sim 5\ m$) and number of samplings along the track (from 20 to 300), as reported in [10].

3 The cluster counting technique

3.1 Conceptual feasibility

The method of primary ionization measurement consists in singling out, in every recorded detector signal, the isolated structures related to the arrival on the anode wire of the electrons belonging to a single ionization act. In order to achieve this goal, special experimental conditions must be met: pulses from electrons belonging to different clusters must have a little chance of overlapping in time and, at the same time, the time distance between pulses generated by electrons coming from the same cluster must be small enough to prevent overcounting. The fulfilment of both these requirements involves imcompatible time resolutions: it appears that the optimal counting condition can be reached only as a result of the equilibrium between the fluctuations of those processes which forbide a full cluster detection efficiency and of the ones enhancing the time separation among different ionization events.

The limit to a full counting efficiency comes from two orders of motivations. The first lies on the specific technology applied for the measurement, that is: the dead time of front-end and of the preprocessing electronic chain, the signal sampling rate, the resolution of the counting algorithm. The above items, which are of critical importance in planning a cluster

counting measurement, will be extensively discussed later on. The second motivation is represented by the physical processes which inherently worsen the detector response. The most relevant ones are the electron attachment and the maximum rate at which the detector can operate.

Electron attachment is a real problem for ionization detection: very small fractions of electronegative pollutant decrease the number of detected electrons considerably. Moreover the attachment probability strongly depends on the electron energy distribution, which has, in a gas, a more complex shape than the usual maxwellian distribution and is very sensitive to gas composition. It follows that an extremely high control of the pollutant level in the gas must be kept during operation.

The maximum rate that a detector can stand without losses of efficiency is related to the time it takes for the gas and the cathodic walls to reabsorbe the positive charges produced in the avalanche process. The electron and positive ion avalanches develop in a well limited region. Electrons quickly recombine on the anode surface and the positive cloud disperses through the slow ion drift toward the cathod. Owing to the little ion mobility ($\mu_{ion} \sim 10^{-3}\mu_{electron}$), the positive charge distribution can locally reduce the electric field, with the result of a gain loss on the collecting wire. A region dense in positive ions around the wire can produce the recombination of a fraction of the electrons from a different avalanche or can capture primary electrons before they reach the amplification region. The spatial spread of the positive ion distribution is small enough to account for local inefficiency only. Therefore this effect is not a relevant problem as long as gas detectors are used as tracking devices. On the other hand, it must be taken into account in a cluster counting measurement where electrons to be detected are closely spaced in distance and time.

The physical process which naturally leads to a primary ionization overestimate is electron diffusion in the gas. Multiple collisions of electrons, coming from a single cluster, on atoms or molecules, in the gas produce a gaussian spread of the arrival time of the electrons on the collecting anode.

The relevant parameters for a cluster counting measurement are *time resolution* τ and *electron diffusion* σ_D. The ideal conditions, which guarantee a real poissonian distribution of the counting, are given by *a time resolution* $\tau = 0$ *in absence of diffusion.* In this way the electrons belonging to the same cluster will reach the anode all at the same time, giving rise to a single structurless signal, whose amplitude is related to the cluster size. The electron arrival times are fixed by the geometrical configuration of the event and by the drift velocity, or, equivalently, by the electric field. A time resolution $\tau \neq 0$ forbids to resolve and count those electron signals which are closer in time than τ. A lack of diffusion and a finite resolving time result in a systematic inefficiency in primary ionization counting. On the other hand a $\sigma_D \neq 0$ determines a spreading of the arrival time for electrons of the same cluster. Therefore, for $\tau = 0$ and $\sigma_D \neq 0$, the number of counted signals is equal the total ionization number in the gas, which is related to the whole energy deposit and so fluctuates according to a Landau-like distribution.

A quality parameter, which allows to discriminate a primary ionization counting from a total energy loss measurement, can be defined as the ratio between the dispersion of the counting around the mean and the square root of the mean: $\xi = \sigma/\sqrt{< N >}$. In an ideal counting, the poisson statistics guarantees $\xi = 1$. For a fixed gas mixture and electrostatic configuration, that is for a given value of σ_D, we expect that the electron counting distributions show a large value of ξ for $\tau = 0$, according to the Landau statistics, which decreases for increasing τ, reaching the value $\xi = 1$ for an optimal value of τ.

Monte Carlo simulations [3] have shown that this occurs when the mean of the counting distribution is equal to the number of primary ionizations generated by the program.

We can conclude that, when the combined effects of diffusion and finite resolution lead to the condition $\xi = 1$, the diffusion exactly compensates the loss of counting due to the finite resolving time, making the electron counting a real primary ionization measurement.

3.2 The advantages of Helium

We propose a technique to measure the primary ionization by counting the pulses, related to the arrival of all electrons from a cluster on the anode wire, within the whole signal recorded in a drift cell. This counting requires a good time resolution, to be determined by the compensation mechanism with electron diffusion, and a low pulse density in the time gate available for signal acquisition, to prevent possible overlaps. The choice of a suitable gas mixture can improve the technical feasibility of the measurement. Helium based gas mixtures, thanks to an increasing popularity in high precision physics because of its long radiation length [11], show many interesting features in connection with cluster counting.

First of all the high ionization potential of Helium, 24.5 eV, compared to Argon, 15.7 eV, causes a smaller primary and total ionization density (in [12] 4.8 $clusters/cm$ and 8 $electrons/cm$ are respectively quoted) and, therefore, a spatial gap between consecutive clusters which is about 6 times larger than the corresponding one in Argon.

On the other hand a small cluster density entails a greater relative sensitivity, for a given resolving time, to variations in cluster deposition. This point is of critical importance in a particle identification measurement, where the informations about the particle momentum, provided by a spectrometer, must be matched with the theoretical expectation for the specific ionization for different masses, in order to assign the right flavour to the particle with a good confidence level.

Furthermore electron drift velocity in helium is smaller than in conventional argon mixtures for every value of the reduced electric field E/p, whereas saturation occurs in argon yet at 300 $V/cm \cdot atm$. A low drift velocity amplifies cluster separation in the time domain, which is of interest for our purposes. A higher ion mobility, entailing a fast clear up of the space charge region, makes helium more attractive than argon in cases where higher gains are required for better spacial resolutions.

Finally the diffusion coefficient in pure helium is greater than in argon, but neverthless a small amount of quencher in the gas reduces the diffusion to a level which is comparable with diffusion in the corresponding argon mixtures [12].

3.3 Technical aspects of the measurement

We want now to evaluate the requirements on the electronics and on the acquisition system necessary for a cluster counting measurement. We establish, therefore, the main features of our ideal detector, in order to derive the foundamental parameters of the measurement setup: the band width of the preamplifier, the sampling rate of the signal and the dynamic range of the ADC for each sampled channel.

We assume that the measurement is done in a 'traditional' drift chamber with a single sense wire cell in a closed configuration (the number of field wires per sense wire is irrelevant at this point). The drift cell is square with a side of 2.6 cm and the chamber is filled with a helium based mixture having a primary ionization density of 10 $clusters/cm$ (small percentages of quencher strongly increase the primary yields) and an average drift velocity, over the cell volume, of 1 $cm/\mu s$.

The drift path differences between two consecutive clusters generated by a track with an impact parameter $b \neq 0$ with respect to the sense wire can be as low as few tens of microns which, at the assumend drift velocity, translate in time separations of a few ns. These typical times require sensitivities of the preamplifier to frequency ranges estending up to at least a few hundred MHz.

Accórding to Nyquest theorem a further factor of two on the sampling rate prevents frequency losses due to the digitization procedure.

The ADC of each channel of the device which samples and records the signal must have a dynamic range large enough to fullfil all physical contraints. Typical cluster population distributions [3] suggest that one must be able to count at least up to 16 electrons within a cluster, which entails 4 *bits*. One needs two more bits to distinguish the relevant signal from noise oscillations with a signal to noise ratio of 4 to 1 and one more bit to take into account the large inherent fluctuations of the avalanche process. We require therefore a minimum of 8 *bit* for the ADC of each sampled channel.

Finally our device must record signals over a time window corresponding to the longest drift path for an electron in the cell.

In summary, in order not to limit experimentally the capabilities of the cluster counting technique, our hypothetical set up will possess the following characteristics:

1. preamplifier highband limit of the order of 1 GHz;
2. sampling frequency of the order of 2 Gs/s;
3. ADC sensitivity of at least 8 *bits*;
4. memory depth for a single event of about 4 $Kbytes$

3.4 Further requests for cluster counting

A realistic planning of a cluster counting measurement requires two additional inputs: 1) a determination of the time resolution, τ_{opt}, which compensate the extracounting produced by the spreading of the arrival times of the electrons belonging to the same cluster due to diffusion; 2) an estimate of the sampling rate, R_{opt}, needed to count with high efficiency the cluster pulses in the whole signal. τ_{opt} depends on b, the impact parameter of the track with respect to the sense wire. It must be averaged over all geometrical configurations.

The evaluation of R_{opt} requires the knowledge of the effective cluster counting algorithm applied in the off-line signal processing. Any algorithm will need a minimum number of bins N_{min} to recognize the shape of the pulse due to a cluster, according to a given cluster definition. The optimal sampling rate is expressed by the relation:

$$R_{opt} = \frac{N_{min}}{\tau_{opt}} \tag{3}$$

A convenient way to obtain a reliable determination of τ_{opt} and R_{opt} is the development of a specific cluster finding algorithm to be applied and tested on a Monte Carlo simulation of the detector, which takes into account all the relevant physical processes.

4 Monte Carlo simulation

4.1 Input parameters

The analyzed drift volume is represented, in cross section, by a 2.6 cm side square cell. The sense wire, 25μm diameter, is set at 1800 V with respect to the cathodic walls, assumed for simplicity continuous. The simulation program reproduces the detector operation taking into account what follows:
a) *Statistical fluctuations in the primary ionization process.* The number of primary ionization is generated, according to a Poissonian law with a mean value N_{cl} per unit length.
b) *Cluster size.* The number of secondary electrons produced in each collision is extracted according to the experimental distribution described in [6].
c) *Electrostatic configuration.* The electrostatic configuration of the cell has been computed with the GARFIELD program [13].
d) *Electrons drift and diffusion.* The values of the drift velocity, v_{drift}, and of the longitudinal diffusion, σ_D, as a function of the electric field, are obtained from a fit to experimental [14] and Monte Carlo [12] determinations for the gas mixtures $90\%He - 10\%iC_4H_{10}$, $95\%He - 5\%iC_4H_{10}$ and $80\%He - 20\%CH_4$. In order to follow the electron path and to compute accurately the arrival time on the sense wire, the local field E is computed over a fine grid 50×50 μm^2. At this phase of the simulation one is able to study the physical processes which affect a general primary ionization counting procedure, with a glance also at the relevant effects originated from the detector geometry (section 4.2). The next step consists in building, from the electron arrival time sequence, a digitized signal which can be processed by a cluster counting algorithm (section 4.3).
e) *Amplification region.* The number of electrons in the avalanche and the total amplitude of the signal on the wire are extracted from a Polya distribution [15].
f) *Pulse trails.* For each electron, the simulated arrival pulse is assumed to have a gaussian shape, of standard deviation σ_r, on the rising front and a double exponential, of time constants τ_{f1} and τ_{f2}, in the falling edge. The rise ($\tau_r = 2\sigma_r = 3.4\ ns$) and the fall times ($\tau_{f1} = 3\ ns$ and $\tau_{f2} = 60\ ns$) are choosen to emulate the typical shape of the isolated pulses observed in real signals which have been acquired in the analogous experimental condition described in section 5: $90\%He - 10\%iC_4H_{10}$ gas mixture, band width of the preamplifier of $0.1 - 1.7\ GHz$, sampling rate $2\ Gs/s$ and digitization 8 *bits* per channel. The pulse trails are generated by adding together the pulses relative to the arrival of each single electron on top of an electronic random noise. The electronics noise amplitude is extracted, according to a gaussian distribution with mean and standard deviation typical of real signals, relative to the same experimental setup as before.
g) *Digitization.* The digitization procedure simulates a sampling rate of $2Gs/s$ and a dynamic range of 8 *bits* per channel.

The simulated signal is compared in fig.(2) to a real signal.

4.2 Resolving time and longitudinal diffusion effects

In order to analyze effects due to the particular geometry, we compare the numbers of counted and generated clusters along a track as a function of its impact parameter (fig.(3)). For small impact parameters ($0.1\ cm \leq b \leq 0.6\ cm$), the counting efficiency decreases with b because of the decreasing differences between the electron path trajectories along the drift direction. For impact parameters in the range $0.6\ cm \leq b \leq 1.2\ cm$, the efficiency increases because of the slower drift velocity in the regions far away from the anode.

Moreover, the spreading of the arrival times, due to diffusion, increases with the drift length and, hence, with the impact parameter.

In order to save the generality of our discussion, in the following we will refer to a set of events where the impact parameter has been randomly extracted from a uniform distribution in the range $0\ cm \leq b \leq 1.3\ cm$.

Let's first consider the case of no diffusion. In this condition the number of clusters arriving at the sense wire is not effected by the cluster size. In Fig.(4,a) the number of counted clusters per unit length is plotted versus the number of generated primary clusters per unit length. Each curve corresponds to a different resolving time τ, in the range $0\ ns \leq \tau \leq 8\ ns$. The effect of the *resolving time* is such that only the electrons arriving at the wire with relative delays greater than τ are counted.

We introduce now the effect of the diffusion. Fig.(4,b) is the analogous of Fig.(4,a) for a σ_D value, proper of the 90% He – 10% iC_4H_{10} mixture. One notices that, for the set of resolving times considered previously, the diffusion blows up the clusters in a way that the number of counted clusters exceedes now the number of generated clusters for small resolving times. Fig.(5) provides a further evidence for the correspondence of the primary ionization measurement to the poissonian behaviour of the counting.

Fig.(6) shows that, for any given cluster density, there is an optimal value of the time resolution τ_{opt}, which reduces the number of counted pulses to the number of total clusters. For $N_{cl} = 12\ /cm$, which is a reasonable value for a $90\%He - 10\%iC_4H_{10}$ mixture. The required time resolution is $\tau_{opt} = 4.0\ ns$.

We stress that this result is related to the detector geometry: it depends on the impact parameter and on the size of the drift cell.

4.3 The counting algorithm

The full digitized event is stored in the array Y(i) where i corresponds to the time T elapsed since the trigger occurrence: i=$T \times f_s$, f_s being the digitizer sampling frequency. A single pulse is characterized by its rise time, T_r, fall time, T_f, and amplitude.

The search for cluster pulses is performed by scanning the array $Y(i)$, suitably filtered to remove random electronics noise, which may generate fake signals, and long tails, which cause pile-up. The local maxima of $Y(i)$ are identified as cluster pulses according to threshold criteria on the amplitude of $Y(i)$ and on its derivative, to consistency criteria on the rise and the fall times of the maxima, T_r and T_f, and to isolation criteria between the maxima and their adjacent minima. All the values for the described criteria are defined by the analysis of a fiducial region of $Y(i)$.

The search algorithm has been applied to Monte Carlo generated signals. Fig.(7) shows, for different cluster densities, the difference between the number of clusters counted with the described algorithm and the number of generated clusters versus the impact parameter for a particular gas.

In order to assert the realiability of the algorithm we have looked at the differences between the electron arrival times as generated in the Monte Carlo and the times at which the algorithm identifies a peak (fig. (8)). The mean value of such a distribution is 7.5 bins, which corresponds to $3.75\ ns$ (to be compared with the rise time of the pulse shape generated, $T_r = 3.4\ ns$). Its standard deviation ($\sigma = 0.4\ ns$) is compatible with the digitizer resolution.

An estimate of the effective resolving time of the algorithm can be obtained by comparing the results given by the algorithm and the number of pulses counted when a resolving

time τ is simulated as described in section 4.2. Fig.(9) shows that the time resolution of the search technique is in the range $2 - 3\,ns$ for cluster density varying from $5\,/cm$ to $28\,/cm$. A different way to study the algorithm performance is illustrated by fig.(10), where the counting efficiency for all the electron pulses in a signal is plotted as a function of the time separation between a pulse and the previous one. The algorithm is not sensitive to signals separated by less than $4\,bins = 2\,ns$. However for time separation greater than $7\,bins = 3.5\,ns$ the efficiency is greater than 70% and it reaches the full efficiency for separations larger than $10\,bins$ ($5ns$).

For $N_{cl} = 12\,/cm$, the algorithm resolution is $\tau \sim 2.5\,ns$ (fig.(9)). Taking into account the simulated $2\,Gs/s$ sampling rate, this time corresponds to a number of bins $N_{min} = 5$, necessary to identify the clusters. We conclude, then, the optimal sampling rate for a gas mixture with $12\,primary\ ionizations/cm$ in the described detector ($2.6 \times 2.6\,cm^2$ square drift cell) is (see section 4.2):

$$R_{opt} = \frac{N_{min}}{\tau_{opt}} = \frac{5}{4.0} \simeq 1.25 Gs/s \tag{4}$$

5 Results from a test beam

In order to test in a real experiment the result of the Monte Carlo study described before, measurement of primary ionization in some mixture of helium-isobutane and helium-methane have been performed [17] with beams of pions and muons at the P.S.I. of Villigen (Zurich, Switzerland) in the $200 - 300\ MeV/c$ range impinging on a test drift tube with the same features of the detector used in the simulation (see section 3.3 and 4). Details on the experimental setup can be found in [16] and [17]. The data have been collected in a not dedicated test beam, therefore the available set of measurement is not complete. It is just intended to represent an evidence of the feasibility of the cluster counting in a conventional drift detector filled with a helium based gas mixture.

The space charge effect, discussed in section 3.1, has been observed in a $95\%He - 5\%iC_4H_{10}$ mixture as a function of the angle α between the beam and the direction perpendicular to the sense wire. A rough estimate of the typical dimension of the spatial charge region, about 500 μm, can be inferred from fig.(11). Even though the effect is relevant only for angles smaller than 30^0, we report about the analysis of data collected with angles of 45^0. Fig. (12) shows two measured distribution of clusters corresponding to different gas mixtures. The very good values of the poissonian quality parameter ξ have been achieved after the application to the data of correction factors obtained from Monte Carlo studies (see fig.7), to eliminate the dependence of the counting efficiency on the impact parameter. In table (1) the quality of the measurement before and after correction is compared for different gas mixtures and different momenta.

5.1 π/μ separation

The rejection power for pion-muon separation has been evaluated for two different values of the beam momentum. In order to obtain a realistic estimate of the results achievable in a large scale experiment, different sets of measurements corresponding to different track lengths have been simulated by adding up events extracted according to the cluster (or dE/dx) distributions in a single cell for the two particle types. The underlying assumption

is that changes and correlations in specific energy loss along the whole path of the particles can be neglected. The set of data used refers to the $95\%He - 5\%iC_4H_{10}$ gas mixture and to beam momenta of 200 and 280 MeV/c. The cluster distributions for single cell and 100 times sampled tracks are shown in fig. 13, while the resolution as a function of the sampling is reported in fig. 14. Fig. 15 shows the best π/μ discrimination achievable by an ideal cluster counting measurement. This has been evaluated by extracting the single cell measurements not from the experimental cluster distribution but from a gaussian fit to it.

The available data sample unfortunately allows us to study the π/μ separation only for two values of the particle momenta: 200 and 280 MeV/c. The overall results for 100 times sampled tracks, sample length 3.7 cm, in $95\%He-5\%iC_4H_{10}$ are plotted in fig. 16 together with theoretical evaluations of the dE/dx resolution with the usual parametrization [1]:

$$\sigma(\%) = 40.7n^{-0.43}l^{-0.32} \tag{5}$$

where n is the total number of samples and l is the sampling length.

5.2 Primary ionization measurement

The total ionization, produced in a gas mixture, is correlated to the specific energy loss by the average energy w required for the production of one electron-ion pair. Neglecting non linear effects, it is possible to consider the total ionization as given by:

$$\left(\frac{dN}{dx}\right)_t = \frac{p_1}{w_1}\left(\frac{dE}{dx}\right)_1 + \frac{p_2}{w_2}\left(\frac{dE}{dx}\right)_2 \tag{6}$$

where p_1 and p_2 are the helium and the hydrocarbon percentages. Analogously, assuming that $< N_e >$ is the mean electron population in each cluster, we can write for the primary ionization:

$$\left(\frac{dN}{dx}\right)_p = \frac{1}{< N_e >_1}\frac{p_1}{w_1}\left(\frac{dE}{dx}\right)_1 + \frac{1}{< N_e >_2}\frac{p_2}{w_2}\left(\frac{dE}{dx}\right)_2 \tag{7}$$

The dE/dx curves, inferred by the Bethe-Bloch parametrization, are superimposed in fig. 17 to the experimental data. The agreement is reasonably good, given the errors. It is possible to determine the cluster density more accurately by taking into account the distribution of clusters for the long tracks as defined in the previous paragraph, for $200MeV/c$ and $280MeV/c$ momentum pions in $95\%He - 5\%iC_4H_{10}$ gas mixture:

$$\delta_{cl,200} = 10.10 \pm 0.50 \; clusters/cm \tag{8}$$

$$\delta_{cl,280} = 9.65 \pm 0.47 \; clusters/cm \tag{9}$$

Expressing equation (7) as:

$$\frac{dN}{dx} = \delta_{cl} = K_1 p_1 \left(\frac{dE}{dx}\right)_1 + K_2 p_2 \left(\frac{dE}{dx}\right)_2 \tag{10}$$

we can fit the best values of the constants K_1 and K_2 obtaining, for minimum ionizing pions:

$$\delta_{cl,He} = 5.5 \pm 0.9 \; clusters/cm \tag{11}$$

$$\delta_{cl,iC_4H_{10}} = 70 \pm 12 \; clusters/cm \tag{12}$$

These values are in good agreement with ref. [12].

6 Conclusions

The reasons which make cluster counting a very promising technique for particle identification purposes have been discussed with a special care to its advantages with respect to the usual dE/dx measurement.

The compensation mechanism, between detector dead time and longitudinal diffusion, has been shown to guarantee the conceptual feasibility of the maesurement, by means of a Monte Carlo study. The technical aspects of cluster counting have also been investigated and the enormous advantages coming from a Helium based mixture are exploited to give a realistic estimate of the necessary performances of the electronics and the digitizing system in a conventional drift cell.

Summarizing, in a square drift cell of $2.6\,cm$ side, as described in section 3, filled with a gas with 12 *primary ionizations/cm* per m.i.p., efficient cluster counting requires a BW of the preamplifier of the order of 500 MHz, a sampling rate of 1.25 Gs/s and an ADC dynamic range of 8 *bits*.

An algorithm for the search of clusters has been developed and shown to represent a realiable tool for the off-line cluster counting analysis.

Finally, a few experimental results, confirming the strength of this approach to particle identification have been presented.

The feasibility of the cluster counting technique is, then, proven from both the experimental and the analysis point of view.

Acknowledgements

We thank the KLOE collaboration which encouraged us to proceed towards a feasibility study of the cluster counting method.

References

[1] A. H. Walenta, IEEE, vol.NS-26, n^0 1 (1979)

[2] Proc. Symp. on the Jesse Effect and Related Phenomena, Gatlinburg (Tenn.) 1973 (Radiat. Res. **59**, 337 (1974))

[3] F. Lapique and F. Piuz, NIM **175** (1980) 297-318

[4] J. H. Cobb, W. W. M. Allison e J. N. Bunch, NIM **133** (1976) 315-323

[5] V. A. Chechin *et al.*, NIM **98** (1972) 577

[6] H. Fitschle *et al.*, NIM **A301** (1991) 202-214

[7] B. Rossi, *High Energy Particles* Prentice-Hall, New York 1952

[8] L. Landau, J. Phys. (USSR) **8** (1944) 201

[9] P. V. Vavilov, Sov. Phys. JEPT **5** (1957) 749

[10] B. Sitar, G. I. Merson, V. A. Chechin, Yu. A. Budagov, *Ionization Measurements in High Energy Physics* Springer-Verlag (1993)

[11] F. Grancagnolo, Proc. Workshop on heavy quarks factory and nuclear physics facility with Superconducting Linacs, Courmayeur, eds. E. De Sanctis, M. Greco, M. Piccolo and S. Tazzari (1987) p. 599
F. Grancagnolo, NIM **A277** (1989) 110

[12] A. Sharma and F. Sauli, CERN-PPE/93-51 10 Febbraio 1993

[13] R. Veenhof, GARFIELD a drift chamber simulation program - Version 3 (1991), CERN Program Library W5050

[14] P. Bernardini *et al. Precise measurements of drift velocities in helium gas mixtures* NIM **A355** (1995) 428-433

[15] G. D. Alkhazov, NIM **89** (1970) 155

[16] G. Cataldi, 'Il problema della separazione π/μ nella camera a *drift* di KLOE', tesi di dottorato, Feb. 1995, Consortium of Universities of Bari and Lecce, *unpublished*
S. Spagnolo, 'La camera a drift di KLOE: definizione dei parametri e misure di ionizzazione primaria in miscele di elio', tesi di laurea, Dec. 1993, University of Lecce, *unpublished*

[17] G. Cataldi *et al. Results from a cluster counting measurement in helium-hydrocarbon mixtures* KLOE note n^0 155 Feb. 1996

Table 1: *Counted clusters before and after the application of a corrective factor.* P_{ee} *is the percentage of events contained in the tail of the distribution after the correction.*

Mixture	p_{beam} MeV/c	N_{cl} $(before)$	ξ $(before)$	N_{cl} $(after)$	ξ $(after)$	P_{ee} %
$80\%He$	280	34.4 ± 6.9	1.18 ± 0.06	33.7 ± 5.6	0.96 ± 0.05	3.3
$20\%CH_4$	400	34.2 ± 6.8	1.16 ± 0.07	33.0 ± 5.7	0.99 ± 0.06	4.4
$95\%He$	200	38.9 ± 9.4	1.51 ± 0.06	37.8 ± 6.4	1.04 ± 0.06	4.9
$5\%iC_4H_{10}$	280	38.8 ± 9.3	1.49 ± 0.03	36.8 ± 6.1	1.01 ± 0.02	5.0
$90\%He$	150	70.8 ± 10.0	1.19 ± 0.07	62.3 ± 8.0	1.01 ± 0.05	5.2
$10\%iC_4H_{10}$	200	49.6 ± 9.4	1.33 ± 0.08	46.8 ± 6.9	1.01 ± 0.06	4.1
	270	46.8 ± 9.5	1.39 ± 0.08	45.7 ± 7.0	1.04 ± 0.06	4.8
$85\%He$	250	57.6 ± 8.2	1.08 ± 0.05	56.6 ± 7.4	0.98 ± 0.04	3.8
$15\%iC_4H_{10}$						

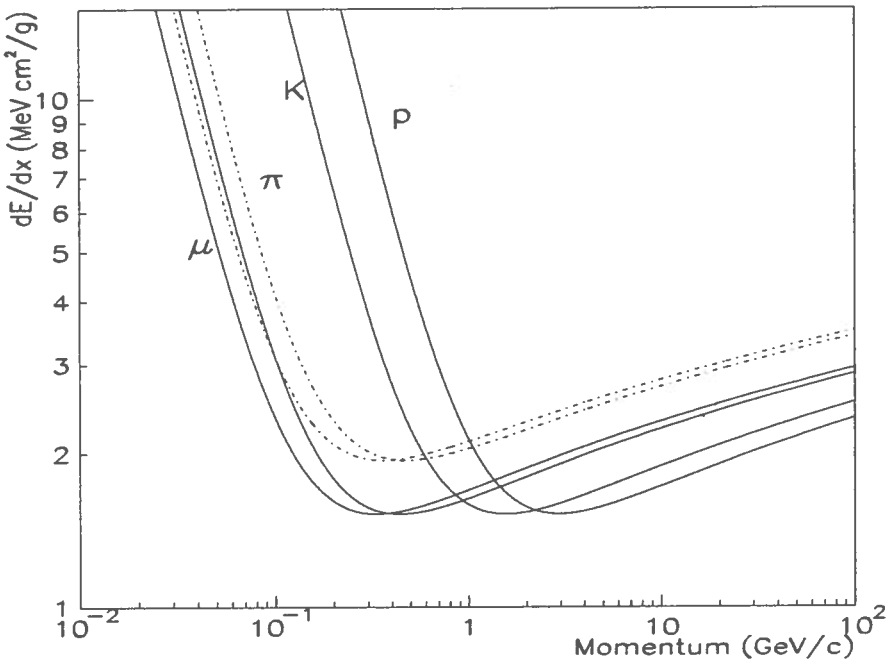

Fig. 1 Energy loss in Argon (solide lines) and in Helium (dash-dot line) for different particles.

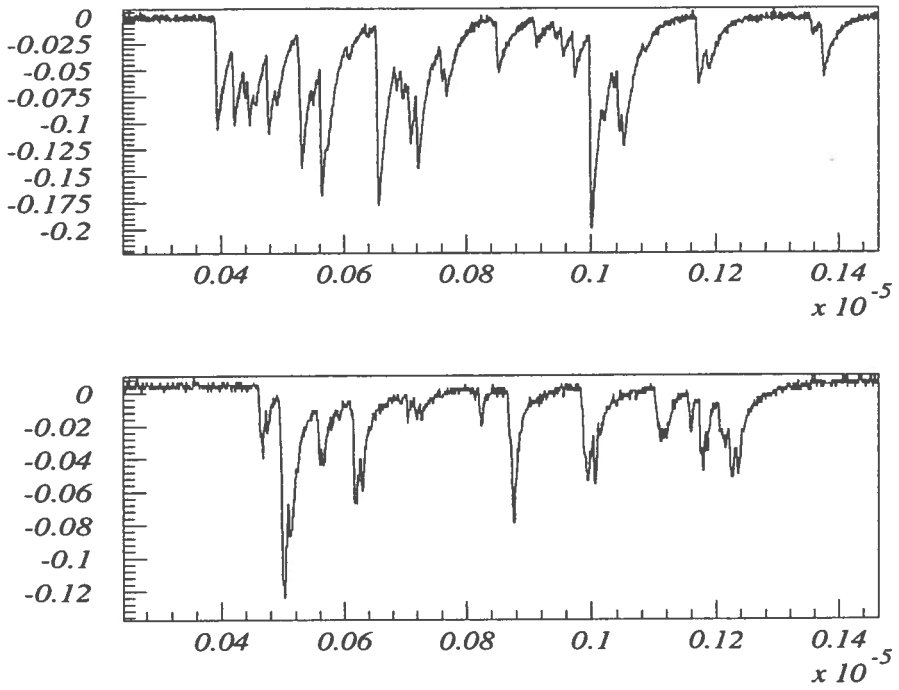

Fig. 2 A simulated signal (top) and a signal acquired in experimental condition very close to the simulated ones (bottom). The horizontal scale is in seconds, the vertical scale is in arbitrary units.

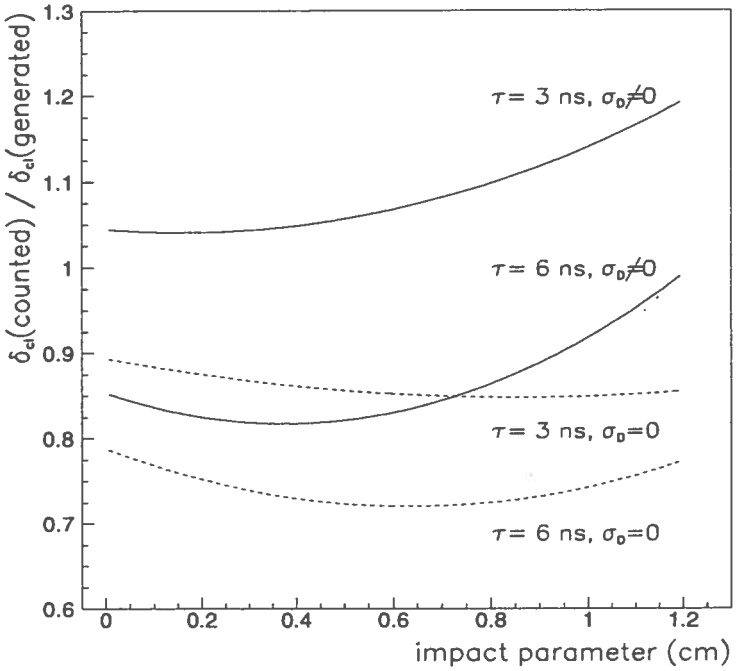

Fig. 3 Counting efficiency, for a cluster density of $N_{cl} = 12$ *clusters/cm*, as a function of the distance of closest approach of the track to the sense wire (impact parameter) for different values of τ and σ_D.

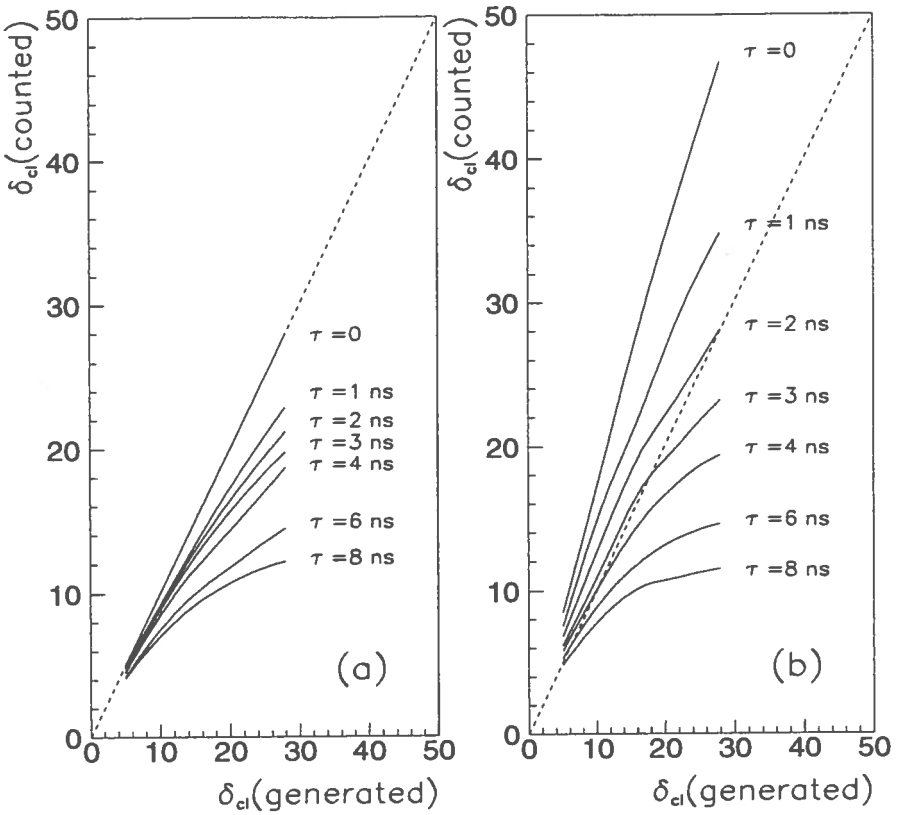

Fig. 4 Counted versus generated clusters with different simulated dead time τ in absense of longitudinal diffusion (a) and for a longitudinal diffusion proper of a $90\%He - 10\%iC_4H_{10}$ mixture (b). The dotted line refers to the ideal counting.

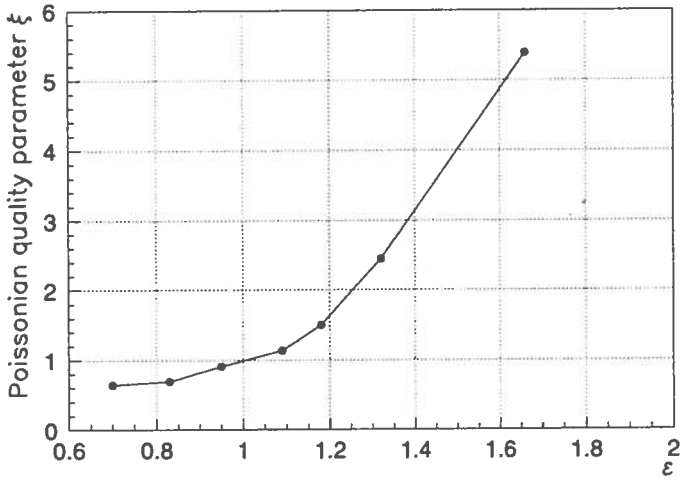

Fig. 5 For a simulated cluster density of $12/cm$ the quality parameter ξ, previously defined, is plotted versus the ratio of counted over generated clusters, ϵ. Each point corresponds to a different simulated dead time.

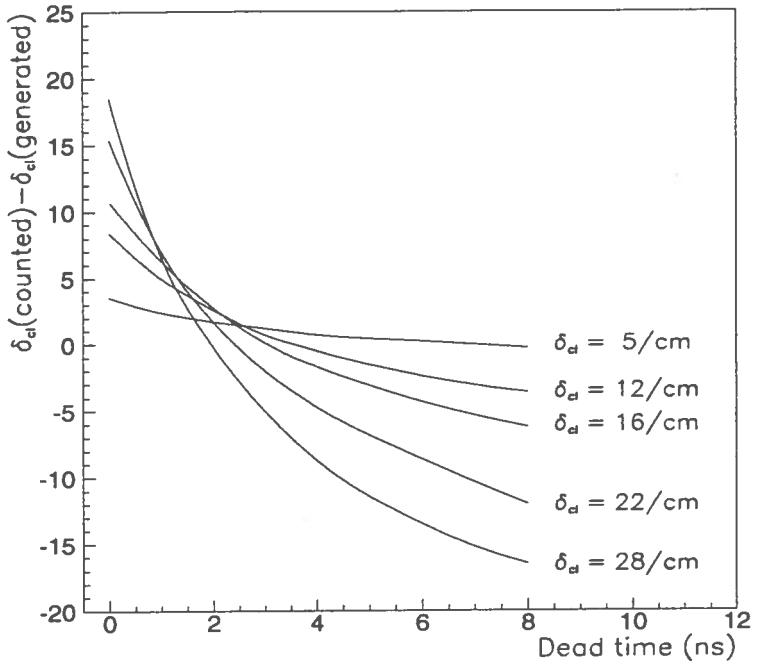

Fig. 6 Difference between counted and generated clusters as a function of the simulated dead time τ. Longitudinal diffusion proper of a $90\%He - 10\%iC_4H_{10}$ mixture.

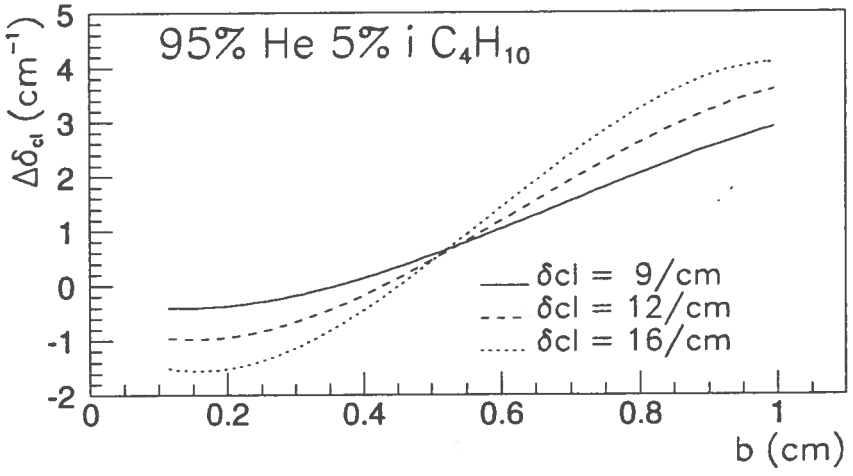

Fig. 7 Difference between the number of counted clusters according to the described algorithm and the generated number of clusters per unit length as a function of the impact parameter for different cluster density.

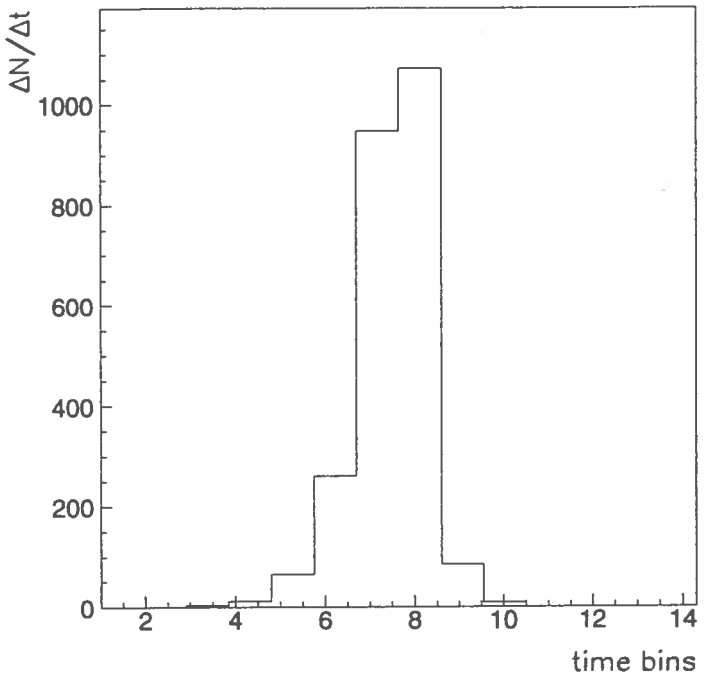

Fig. 8 Distribution of the residues between the arrival time generated in the Monte Carlo and the time at which the search algorithm identifies a clusters.

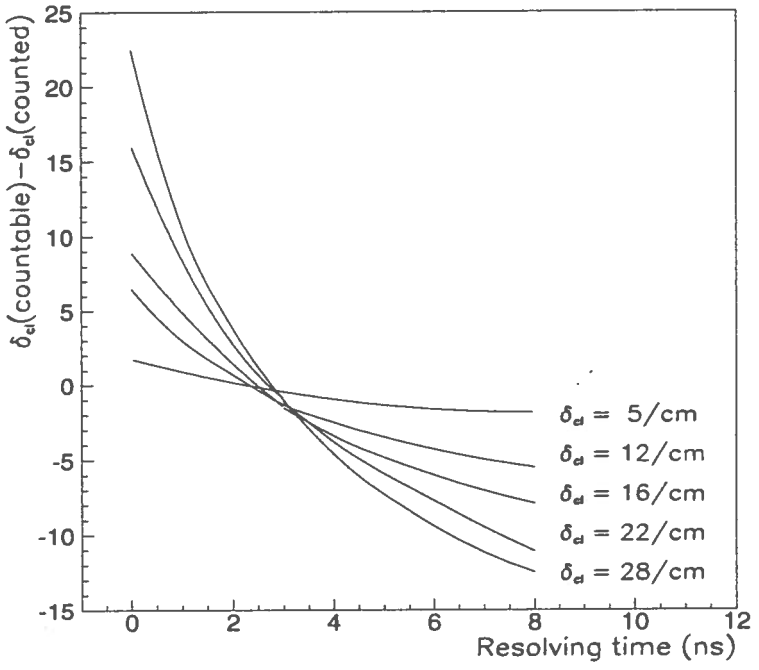

Fig. 9 A comparison between the number of clusters counted by the search algorithm and the counting corresponding to a simulated time resolution.

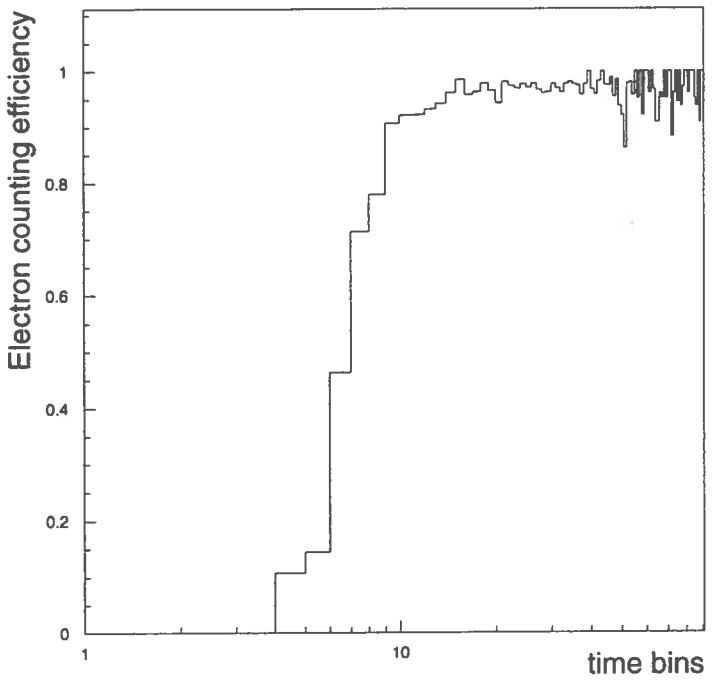

Fig. 10 The algorithm efficiency for resolving peaks versus the distance (in bins) of each pulse from the previous one.

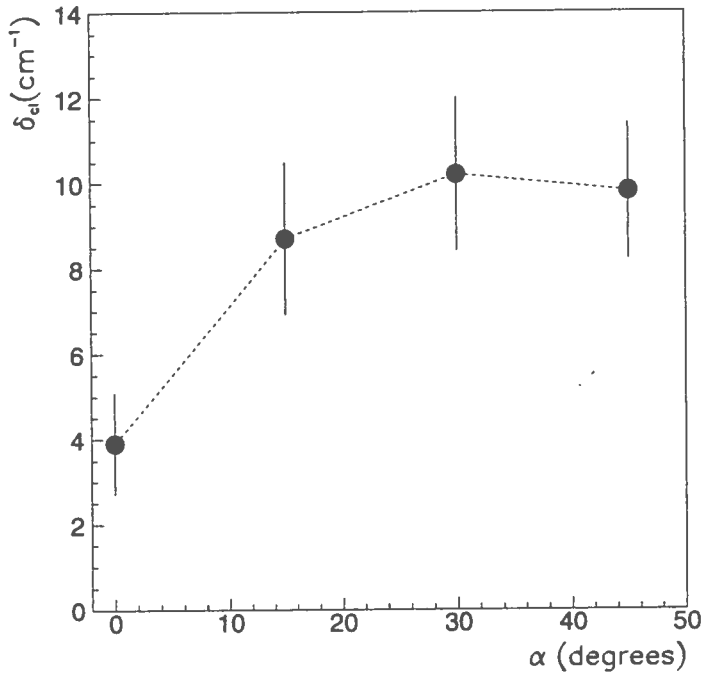

Fig. 11 Clusters density, δ_{cl}, as a function of the angle α between the track and the normal to the tube for a $25\mu m$ wire diameter. The gas mixture used is $95\%He - 5\%i\,C_4H_{10}$.